



Title	Surface morphologies and magnetic properties of Fe and Co magnetic thin films on polyethylene naphthalate organic substrates
Author(s)	Kaiju, Hideo; Abe, Taro; Kondo, Kenji; Ishibashi, Akira
Citation	Journal of Applied Physics, 111(7), 07C104 https://doi.org/10.1063/1.3670609
Issue Date	2012-04-01
Doc URL	http://hdl.handle.net/2115/49377
Rights	Copyright 2012 American Institute of Physics. This article may be downloaded for personal use only. Any other use requires prior permission of the author and the American Institute of Physics. The following article appeared in J. Appl. Phys. 111, 07C104 (2012) and may be found at https://dx.doi.org/10.1063/1.3670609
Type	article
File Information	JAP111-7_07C104.pdf



[Instructions for use](#)

Surface morphologies and magnetic properties of Fe and Co magnetic thin films on polyethylene naphthalate organic substrates

Hideo Kaiju, Taro Abe, Kenji Kondo, and Akira Ishibashi

Citation: *J. Appl. Phys.* **111**, 07C104 (2012); doi: 10.1063/1.3670609

View online: <http://dx.doi.org/10.1063/1.3670609>

View Table of Contents: <http://jap.aip.org/resource/1/JAPIAU/v111/i7>

Published by the [American Institute of Physics](http://www.aip.org).

Related Articles

Origin of magneto-optic enhancement in CoPt alloys and Co/Pt multilayers

Appl. Phys. Lett. **100**, 232409 (2012)

Reproducible domain wall pinning by linear non-topographic features in a ferromagnetic nanowire

Appl. Phys. Lett. **100**, 232402 (2012)

L10-FePt based exchange coupled composite films with soft [Co/Ni]N multilayers

J. Appl. Phys. **111**, 103916 (2012)

Transport and magnetic properties of the Co₂MnSi/Al/Co₂MnSi trilayer

Appl. Phys. Lett. **100**, 222407 (2012)

Spin-orbit field switching of magnetization in ferromagnetic films with perpendicular anisotropy

Appl. Phys. Lett. **100**, 212405 (2012)

Additional information on J. Appl. Phys.

Journal Homepage: <http://jap.aip.org/>

Journal Information: http://jap.aip.org/about/about_the_journal

Top downloads: http://jap.aip.org/features/most_downloaded

Information for Authors: <http://jap.aip.org/authors>

ADVERTISEMENT



Special Topic Section:
PHYSICS OF CANCER

Why cancer? Why physics? [View Articles Now](#)

Surface morphologies and magnetic properties of Fe and Co magnetic thin films on polyethylene naphthalate organic substrates

Hideo Kaiju,^{1,2,a)} Taro Abe,¹ Kenji Kondo,¹ and Akira Ishibashi¹

¹Laboratory of Quantum Electronics, Research Institute for Electronic Science, Hokkaido University Sapporo, Hokkaido, 001-0020, Japan

²PRESTO, Japan Science and Technology Agency, Kawaguchi, Saitama 332-0012, Japan

(Presented 2 November 2011; received 13 September 2011; accepted 13 October 2011; published online 9 February 2012)

We have studied the surface morphologies and magnetic properties of Fe and Co thin films evaporated on polyethylene naphthalate (PEN) organic substrates toward the fabrication of spin quantum cross devices. As a result, the surface roughnesses of Co (6.1 nm)/PEN and Co (12 nm)/PEN are as small as 0.1 and 0.09 nm, respectively, corresponding to less than one atomic layer, in the same scanning scale as the thickness. As for the magnetic properties, the coercive force of the Co/PEN shows the constant value of 2 kA/m upon decreasing the Co thickness from 35 to 10 nm, and it increases up to 7 kA/m upon decreasing the Co thickness from 10 to 5 nm. It decreases when the Co thickness is less than 5 nm. These results can be explained by the competition between the shape magnetic anisotropy and the induced magnetic anisotropy. © 2012 American Institute of Physics. [doi:10.1063/1.3670609]

Molecular spintronics has attracted an extensive amount of interest since the discovery of the magnetoresistance (MR) effect in ferromagnetic-metal/molecules/ferromagnetic-metal junctions.^{1–6} Recently, we have proposed spin quantum cross (SQC) devices, in which molecules are sandwiched between two edges of magnetic thin films deposited on organic substrates with their edges crossed.^{7,8} In SQC devices, the junction area can be scaled down to dimensions of a few nanometers because the thickness of magnetic thin films is determined by the growth rate, ranging from 0.01 to 1.0 nm/s. According to our recent calculation within the framework of the Anderson model, SQC devices exhibit a giant MR effect at room temperature.⁹ In this paper, toward the fabrication of SQC devices, we have investigated the surface morphologies and magnetic properties of Fe and Co thin films evaporated on polyethylene naphthalate (PEN) organic substrates and discussed their feasibility of use in SQC devices.

The Fe and Co thin films were thermally evaporated on PEN organic substrates (10 mm length, 2 mm width, 25 μ m thickness) under a magnetic field in a high vacuum chamber at a base pressure of $\sim 10^{-8}$ Torr. The PEN organic substrates (Teonex Q65) were supplied by Teijin DuPont, Japan. The pressure during the evaporation was 10^{-5} Torr and the growth rate was 1.5–2.5 nm/min at an evaporation power of 400–450 W. The magnetic field for the formation of the induced magnetic anisotropy was 30 kA/m, which was applied in the in-plane transverse direction of the Co and Fe thin films. The surface morphologies of the samples were analyzed by atomic force microscope (AFM; Nanonavi IIs, SII NanoTechnology). The magnetization curves were measured by focused magneto-optic Kerr effect equipment (Neoark, BH-PI920-HU) under a magnetic field up to 40 kA/m at room temperature.

Here, the surface roughness, R_a , is defined by $R_a = 1/L_x L_y \int_0^{L_x} \int_0^{L_y} |h(x,y)| dx dy$, where $h(x,y)$ is the height profile as a function of x and y and $L_{x(y)}$ is the lateral scanning size in the $x(y)$ direction. Figure 1(a) shows the surface roughness as a function of the metal film thickness for Fe/PEN, Co/PEN, and Au/PEN. The surface roughness increases up to 3.8 nm for a film thickness of 21 nm for Au/PEN, whereas the surface roughness decreases down to 0.77 and 0.58 nm with increasing the film thickness up to 40 nm for Fe/PEN and Co/PEN, respectively. Here, we consider the growth mechanism of the Fe/PEN and Co/PEN, and discuss their feasibility in SQC devices from the viewpoint of the surface roughness. Figures 1(b) and 1(c) show the scaling properties of the surface roughness for PEN, Fe/PEN, and Co/PEN. The inset represents the scaling properties of the root mean square (RMS) surface roughness, R_q . The RMS surface roughness obeys a scaling law, $R_q = w(L) \propto L^\alpha$, where $w(L)$ is the interface width corresponding to the standard deviation of the surface height, L is the system size, and α is the growth scaling exponent. From the inset in Figs. 1(b) and 1(c), the growth scaling exponent, α , of PEN is found to be 0.63, which is almost the same value as 0.62 of the Fe (7.8 nm)/PEN. This result indicates that the surface morphology of PEN exhibits almost the same behavior as that of the Fe (7.8 nm)/PEN. In contrast, the growth scaling exponents, α , of Fe (14 nm)/PEN, Co (6.1 nm)/PEN, and Co (12 nm)/PEN are 0.71–0.73, which are different from those of both PEN and Fe (7.8 nm)/PEN. That means that the surface morphologies of Fe (14 nm)/PEN, Co (6.1 nm)/PEN, and Co (12 nm)/PEN are different from those of PEN and Fe (7.8 nm)/PEN. This difference affects their magnetic properties. The relation between the surface morphologies and magnetic properties will be discussed later. Here, we consider their feasibility in SQC devices from the viewpoint of the surface roughness. Since the junction area in SQC devices is determined by the film thickness, the surface

^{a)}Electronic mail: kaiju@es.hokudai.ac.jp.

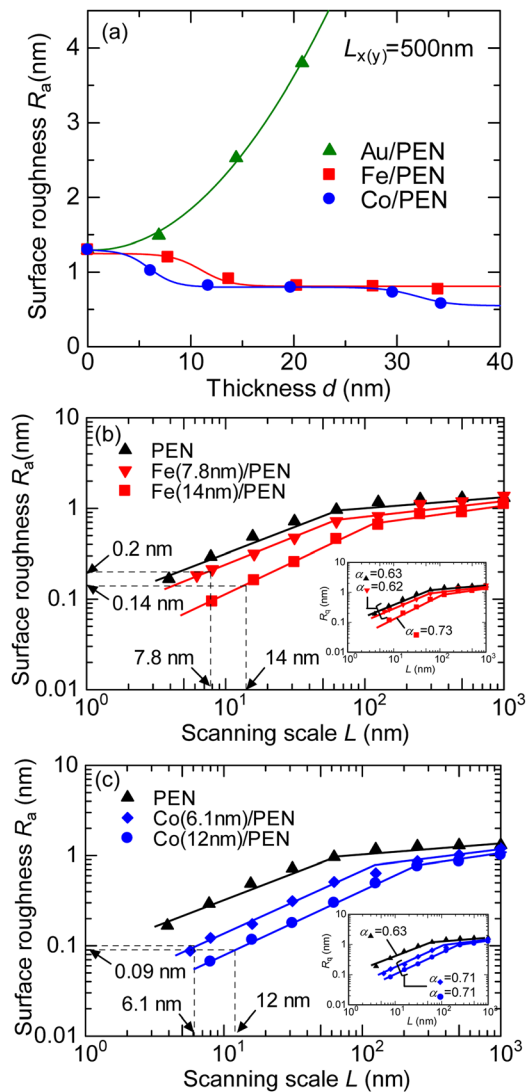


FIG. 1. (Color online) (a) Surface roughness as a function of the metal film thickness for Fe/PEN, Co/PEN, and Au/PEN and the scaling properties of the surface roughness for (b) PEN, Fe (7.8 nm)/PEN, and Fe (14 nm)/PEN, and (c) PEN, Co (6.1 nm)/PEN, and Co (12 nm)/PEN. The inset shows the scaling properties of the RMS surface roughness.

roughness needs to be smooth enough in the same scanning scale as the thickness size. As shown in Fig. 1(b), the surface roughnesses of Fe (7.8 nm)/PEN and Fe (14 nm)/PEN are 0.2 and 0.14 nm, corresponding to one atomic layer, in the scanning scale of 7.8 and 14 nm, respectively. The surface roughnesses of Co (6.1 nm)/PEN and Co (12 nm)/PEN are also as small as 0.1 and 0.09 nm, corresponding to less than one atomic layer, in the scanning scale of 6.1 and 12 nm. These facts indicate that Fe/PEN and Co/PEN are suitable for magnetic metal thin films on organic substrates used for SQC devices from the viewpoint of surface morphologies.

Figure 2 shows the Fe and Co thickness dependences of the magnetization curves for Fe/PEN and Co/PEN. The magnetic field is applied in the transverse direction of each film, which is parallel to the induced magnetic anisotropy axis. In Fig. 2(a), the coercive force of Fe/PEN decreases from 6.1 to 0.57 kA/m upon decreasing the Fe thickness from 22 to 7.8 nm. In comparison, in Fig. 2(b), the coercive force of Co/PEN shows the maximum value of 6.1 kA/m at a Co

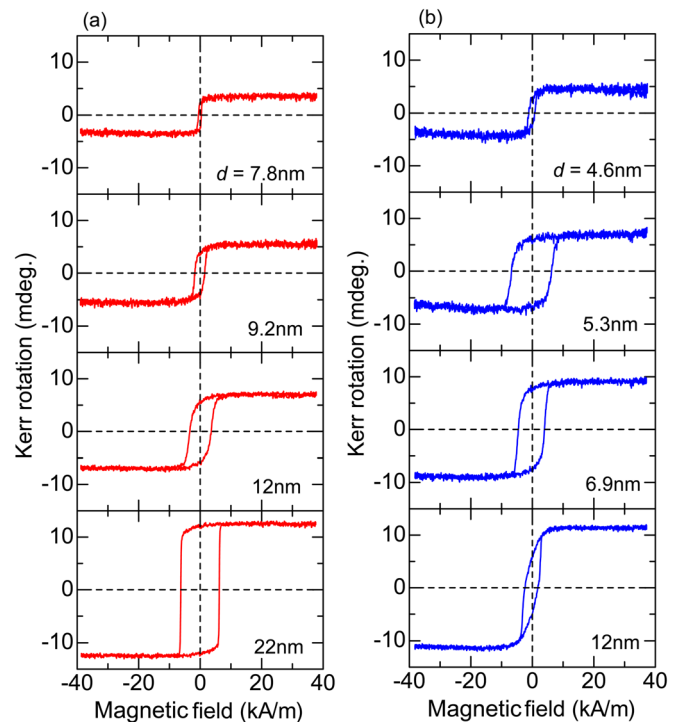


FIG. 2. (Color online) Fe and Co thickness dependences of the magnetization curves for (a) Fe/PEN, and (b) Co/PEN.

thickness of 5.3 nm. This tendency can also be seen in the squareness of the hysteresis loop, M_r/M_s , where M_r and M_s are the residual and saturation magnetization, respectively. The squareness of the Fe/PEN decreases from 0.96 to 0.66 upon decreasing the Fe thickness from 22 to 7.8 nm. The squareness of the Co/PEN shows the maximum value of 0.84 at a Co thickness of 5.3 nm. Figure 3(a) shows the Fe and Co thickness dependences of the coercive force for Fe/PEN and Co/PEN. As already shown in Fig. 2(a), the coercive force of Fe/PEN decreases upon decreasing the Fe thickness and it becomes 0 kA/m at an Fe thickness of 7 nm. The coercive force of the Co/PEN shows the constant value of 2 kA/m upon decreasing the Co thickness from 35 to 10 nm and increases up to 7 kA/m upon decreasing the Co thickness from 10 to 5 nm. It decreases when the Co thickness is less than 5 nm. Here, we discuss the reason why this peak occurs for Co/PEN. First, we examine the coercive force in stage I (Co thickness, $d_{Co} = 10\text{--}35$ nm), as shown in Fig. 3(a). In each illustration of stages I-III in Fig. 3(a), the solid arrow and the dotted arrow represent a strong and a weak magnetic anisotropy, respectively. As is well known, Co thin films have a strong shape magnetic anisotropy. Therefore, the shape magnetic anisotropy, K_s (represented by a solid green arrow) dominates within the total magnetic anisotropy in stage I, where it can be neglected that both the Co surface roughness ($R_a = 0.58\text{--}0.82$ nm for $d_{Co} = 10\text{--}35$ nm in $L_{x(y)} = 500$ nm) and the PEN surface roughness ($R_a = 1.3$ nm in $L_{x(y)} = 500$ nm), shown in Fig. 1(a), affect the Co film shape. This qualitative picture is surely supported by the fact that the coercive force and the squareness of Co (21 nm)/PEN are as small as 2.1 kA/m and 0.37, respectively, when the magnetic field is applied in the transverse direction of Co/PEN, shown in Fig. 3(b), whereas the coercive force and

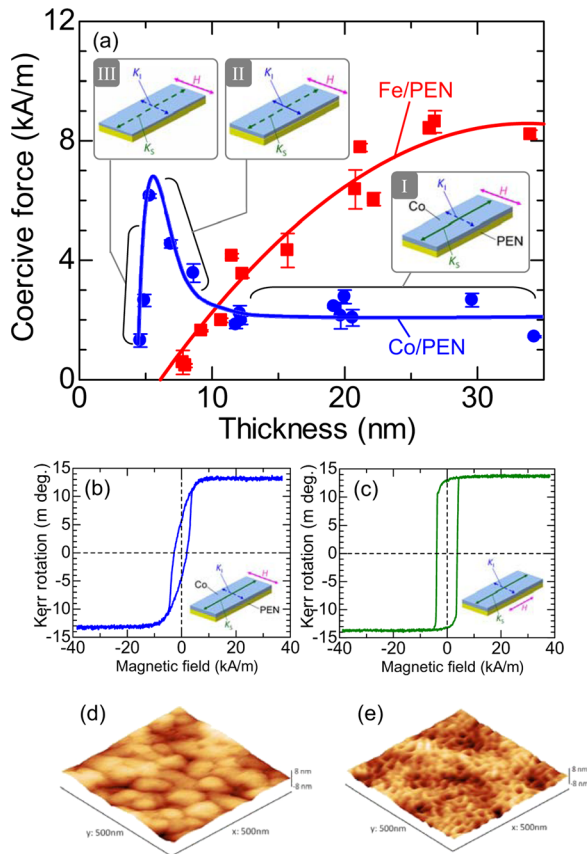


FIG. 3. (Color online) (a) Fe and Co thickness dependences of the coercive force for Fe/PEN and Co/PEN, the magnetization curves with the application of (b) the transverse, and (c) the longitudinal, magnetic field for Co (21 nm)/PEN, and the surface morphologies of (d) Co (6.1 nm)/PEN and (e) Fe (7.8 nm)/PEN.

the squareness of Co (21 nm)/PEN are as large as 4.0 kA/m and 0.94, respectively, when the magnetic field is applied in the longitudinal direction of Co/PEN, as shown in Fig. 3(c). This result means that the magnetic easy axis is almost perpendicular to the external magnetic field. Therefore, the coercive force of the Co films in stage I for Co/PEN has decreased. Next, in stage II ($d_{Co} = 5\text{--}10\text{ nm}$), the Co surface roughness ($R_a = 1.0\text{ nm}$ for $d_{Co} = 5\text{--}10\text{ nm}$ in $L_{x(y)} = 500\text{ nm}$) and the PEN surface roughness ($R_a = 1.3\text{ nm}$ in $L_{x(y)} = 500\text{ nm}$) are considered to affect the Co film shape since the ratios of the Co and PEN surface roughness to the Co thickness are as large as 0.23–0.46. For this reason, the shape magnetic anisotropy, K_s (represented by the dotted green arrow), becomes smaller than the induced magnetic anisotropy, K_I (represented by the solid blue arrow). Therefore, the induced magnetic anisotropy, K_I , dominates within the total magnetic anisotropy. This means that the magnetic easy axis becomes almost parallel to the external magnetic field. This results in the increase of the coercive force and the squareness. Here, it should be noted that the mound-like surface can be seen for Co (6.1 nm)/PEN, as shown in Fig. 3(d). This means that Co thin films can be self-organized even though Co films are quite thin. In contrast, the fiber-like surface can

be observed for Fe (7.8 nm)/PEN, as shown in Fig. 3(e). This fiber-like surface is almost the same as the morphology of the PEN. This means that Fe thin films cannot be self-organized. This result is in good agreement with the fact that the growth scaling exponent, α , of PEN is almost the same value as that of Fe (7.8 nm)/PEN, as shown in the inset of Fig. 1(b). Moreover, this is consistent with the fact that the coercive force becomes 0 kA/m at an Fe thickness of 7 nm, as shown in Fig. 3(a), due to little magnetic interaction between the Fe-Fe grains. Finally, in stage III ($d_{Co} < 5\text{ nm}$), since the formation of Co thin films are quite similar to that of Fe thin films in the Fe(7.8 nm)/PEN shown in Fig. 3(e), the coercive force approaches 0 kA/m. Thus, the peak in the coercive force for Co/PEN can be explained by the competition between the shape magnetic anisotropy and the induced magnetic anisotropy. These results also indicate that Co/PEN films with a Co thickness of 5–10 nm are suitable for the electrodes of SQC devices because a large coercive force and a high squareness of the hysteresis loop are required in SQC devices. In conclusion, Co/PEN films are good candidates for the electrodes of SQC devices, especially with a 5–10 nm junction size, from the viewpoint of the surface morphologies and magnetic properties.

This research has been partially supported by the Management Expenses Grants for National Universities Corporations and a Grant-in-Aid for Young Scientists from The Ministry of Education, Culture, Sports, Science and Technology (MEXT), Precursory Research for Embryonic Science and Technology program from the Japan Science and Technology Agency (JST), and a Grant-in-Aid for Scientific Research from the Japan Society for the Promotion of Science (JSPS). The authors would like to express their sincere appreciation to Dr. M. Hirasaka of Teijin Ltd., Research Manager K. Kubo of Teijin DuPont Films Japan, Ltd., Professor Y. Hirotsu and Associate Professor M. Ishimaru at Osaka University, Professor M. Yamamoto, Assistant Professor K. Matsuda, and M. Takei at Hokkaido University for their cooperation and helpful discussions.

- ¹Z. H. Xiong, D. Wu, Z. V. Vardeny, and J. Shi, *Nature (London)* **427**, 821 (2004).
- ²T. S. Santos, J. S. Lee, P. Migdal, I. C. Lekshmi, B. Satpati, and J. S. Moodera, *Phys. Rev. Lett.* **98**, 016601 (2007).
- ³V. Dediu, L. E. Hueso, I. Bergenti, A. Riminucci, F. Borgatti, P. Graziosi, C. Newby, F. Casoli, M. P. De Jong, C. Taliani, and Y. Zhan, *Phys. Rev. B* **78**, 115203 (2008).
- ⁴F. J. Wang, C. G. Yang, Z. V. Vardeny, and X. G. Li, *Phys. Rev. B* **75**, 245324 (2007).
- ⁵W. Xu, G. J. Szulczewski, P. LeClair, I. Navarrete, R. Schad, G. Miao, H. Guo, and A. Gupta, *Appl. Phys. Lett.* **90**, 072506 (2007).
- ⁶C. Barraud, P. Seneor, R. Mattana, S. Fusil, K. Bouzehouane, C. Deranlot, P. Graziosi, L. Hueso, I. Bergenti, V. Dediu, F. Petroff, and A. Fert, *Nat. Phys.* **6**, 615 (2010).
- ⁷H. Kaiju, A. Ono, N. Kawaguchi, and A. Ishibashi, *Jpn. J. Appl. Phys.* **47**, 244 (2008).
- ⁸K. Kondo and A. Ishibashi, *Jpn. J. Appl. Phys.* **45**, 9137 (2006).
- ⁹K. Kondo, H. Kaiju, and A. Ishibashi, *J. Appl. Phys.* **105**, 07D522 (2009).